View metadata, citation and similar papers at core.ac.uk
brought to you by CORE
provided by Aberdeen University Research Archive

Soil Biology & Biochemistry 49 (2012) 4–10

Contents lists available at SciVerse ScienceDirect

Soil Biology & Biochemistry

journal homepage: www.elsevier.com/locate/soilbio

Rapid incorporation of carbon from ectomycorrhizal mycelial necromass into soil fungal communities

B. Drigo [a], I.C. Anderson [a], G.S.K. Kannangara [b], J.W.G. Cairney [a], D. Johnson [c,*]

[a] Hawkesbury Institute for the Environment, University of Western Sydney, NSW, Australia
[b] School of Natural Sciences, University of Western Sydney, NSW, Australia
[c] Institute of Biological and Environmental Sciences, Cruickshank Building, University of Aberdeen, UK

ARTICLE INFO

Article history:
Received 14 December 2011
Received in revised form
1 February 2012
Accepted 5 February 2012
Available online 20 February 2012

Keywords:
Ectomycorrhiza
^{13}C-mycelium
DNA-SIP
NMR
qPCR
Carbon turnover
Decomposition
Pisolithus microcarpus

ABSTRACT

Ectomycorrhizal mycelial necromass is an important source of carbon for free-living microorganisms in forest soils, yet we know little either of its fate when it enters soil or of the identity of microbes that are able to utilise mycelium as their energy source. Here we used ^{13}C-labelled mycelium of the ectomycorrhizal fungus *Pisolithus microcarpus* in laboratory incubations in combination with DNA-stable isotope probing (SIP) to determine the identity of functionally active soil fungi that can utilise dead mycelium. We also used solid-state nuclear magnetic resonance (NMR) spectroscopy to detect parallel changes in the abundance of key biochemical constituents of soil. A decrease in bulk soil ^{13}C concentration together with rapid loss of glycogen and chitin-glucan during the 4 week incubations suggested that dead mycelium was rapidly turned over. Further, ^{13}C was incorporated into fungal DNA within 7 days of addition to soil. DNA-SIP also revealed a dynamic community of functionally active soil fungi. By applying DNA-SIP and NMR in parallel, our data show that carbon from decaying ectomycorrhizal mycelium is rapidly transformed and incorporated into free-living soil fungi. This finding emphasises that dead extra-matrical mycelium is an important source of labile carbon for soil microorganisms.

© 2012 Elsevier Ltd. Open access under CC BY license.

1. Introduction

Extra-matrical mycelium (EMM) is a key component of the mycorrhizal fungal symbiosis, which is responsible for foraging and actively acquiring scarce nutrients in soil. Regardless of mycorrhizal type, the length of mycelium in soils is vast and is a significant sink for plant assimilates. In forests, the EMM of ectomycorrhizal (ECM) fungi accounts for approximately 30% of microbial biomass (Högberg and Högberg, 2002), about half of the standing fungal biomass (Bååth et al., 2004), and contributes up to 25% of soil CO_2 efflux (Heinemeyer et al., 2007). ECM mycelium can grow to produce several hundred metres of hyphae per gram of soil (Leake et al., 2004) allowing soil derived carbon (C) to be rapidly allocated to EMM, particularly to the actively foraging growth fronts colonising soil organic matter (SOM; Leake, 2001). Extra-matrical mycelium can comprise up to 80% of the biomass of an ECM fungus (Wallander et al., 2001), although this is dependent on functional type (Agerer, 2001). Some ECM fungi generally produce little external mycelium whilst others, such as *Pisolithus* species, produce thick, long-ranging rhizomorphs. The length of hyphae produced by some species enables them to connect host plants to form extensive common mycelial networks (Beiler et al., 2008).

Despite the ecological significance of mycorrhizal mycelium we know remarkably little about the rate of mycelial turnover, or the fate of C contained in hyphal biomass once it dies. The latter issue is particularly important because, when detached from root tips, external mycorrhizal mycelium becomes a large resource of both labile and recalcitrant C that can fuel the activity of soil free-living microorganisms and contribute to the formation of SOM. For example, in a poplar plantation, ECM mycelium was the dominant pathway (62%) through which C entered the SOM pool, exceeding the input via leaf litter and fine root turnover (Godbold et al., 2006). Use of mesh in-growth bags suggests that ECM mycelium has a mean residence time of about 10 years (Wallander et al., 2004), but this is likely to differ based on a number of factors including fungal species, morphology and edaphic conditions.

Whilst it is clear that decaying ECM hyphae contribute to formation of SOM, little is known about the dynamics of specific chemical constituents. The application of solid-state cross polarization/magic angle spinning ^{13}C nuclear magnetic resonance spectroscopy (CP/MAS ^{13}C NMR) to the decaying ECM hyphae in soil

* Corresponding author. Tel.: +44 1224 273857.
E-mail address: d.johnson@abdn.ac.uk (D. Johnson).

0038-0717 © 2012 Elsevier Ltd. Open access under CC BY license.
doi:10.1016/j.soilbio.2012.02.003

opens up possibilities to gain a more complete understanding of the dynamics of C in mycelium *in situ*. Previous studies on soils incubated with uniformly labelled ^{13}C-glucose as substrate have demonstrated that microbial activity is responsible for the accumulation of polymethylene carbons in soils (Baldock et al., 1990). Fungal cell walls contain chitin, β-glucans and proteins, and many of these groups are amenable to analysis with NMR-based techniques. For example, solid-state ^{13}C NMR spectroscopy was used recently to characterise the dynamics of C loss from decomposing culturable soil microorganisms (Fan et al., 2009). The ^{13}C NMR spectral data for α-chitin, chitosan and β-glucans have also been reported (Heux et al., 2000). Thus, there is potential to use these techniques to study in more detail the changes in the abundance of specific chemical constituents of external mycorrhizal mycelium when it dies and is incorporated into bulk soil.

Both the speed at which dead mycelium decays and the factors controlling this in soils are poorly understood and even contradictory. For example, recent analyses suggest a key role of the nitrogen content of hyphae (Koide and Malcolm, 2009), while in other work, no such relationship was found (Wilkinson et al., 2011). The latter found that hyphal necromass rapidly stimulated microbial activity and that this was exaggerated by the effects of species richness of the dead fungi. This finding suggested that some nutrient resources in hyphae were being degraded preferentially by saprotrophic microbes; a similar situation has been found following additions of dissolved organic C (Cleveland et al., 2007; Chigineva et al., 2009). Recent evidence has also shown that saprotrophic fungi can respond rapidly to inputs of EMM (Lindahl et al., 2010). These studies indicate the need to better understand the link between C inputs from EMM and soil biodiversity. This aim is potentially achievable using stable isotope probing (SIP; Radajewski et al., 2000) and has recently been achieved in the context of plant litter inputs. For example, ^{13}C-labelled cellulose was used as a proxy for plant litter inputs to demonstrate how land management practices, such as burning, affect fungal activity (Bastias et al., 2009). This approach has the advantage of utilising commercially available substrates that are highly ^{13}C-enriched in order to maximise the chance of detecting movement of C into nucleic acids. More recently, ^{13}C-enriched rice residues were used to determine the temporal dynamics of C movement into soil bacterial communities throughout 56-days incubation (Lee et al., 2011). These recent developments demonstrate potential for using ^{13}C-enriched necromass as a tracer to determine the fate of fungal C into microbial communities. Indeed, it has recently been suggested that the large biomass of hyphae produced by ECM fungi, along with the ability of many species to grow in culture, provides opportunities to utilise SIP in this context (Kennedy, 2010). Here, we use SIP under controlled laboratory conditions to test the hypothesis that C from decomposing ECM mycelium is rapidly incorporated into soil fungal communities. We combine this approach with parallel measurements of the chemical composition of the soils using solid-state NMR to test whether specific components of hyphal necromass are degraded at different rates.

2. Materials and methods

2.1. Experimental set-up

Soil was sampled to a depth of 5 cm from the surface horizons of a *Eucalyptus*-dominated native forest near the Hawkesbury River in western Sydney, Australia (33°36′40″ S, 150°44′26.5″ E). The soil was a sandy loam with an alluvial formation of low organic matter content (0.7%) and low to moderate fertility (available P, 8 mg kg^{-1}; exchangeable cations: K, 0.19; Ca, 1.0; Mg, 0.28 meq 100 g^{-1}). The soil was sieved (2 mm) and 20 g fwt packed into a total of 12 plastic specimen jars (50 cm^3) and wetted to 10% volumetric water content (dwt). Mycelium of the ECM basidiomycete *Pisolithus microcarpus* (isolate KC2.18) was grown in liquid culture in Petri dishes containing modified Melin-Norkrans (MMN) medium (Marx, 1969). For half of the plates, ^{12}C-glucose (0.5%) was substituted with 99 atom % ^{13}C-glucose as the sole C source (Cambridge Isotope Laboratories, Andover, MA, USA) to produce fungal biomass with ~99% of its C as ^{13}C. Once mycelium had filled the dishes, they were filtered, air dried and lightly homogenised (for *ca* 5 s) with a glass tissue homogeniser. The mycelium was mixed into the soil (145 mg dwt of mycelium per jar) to create two treatments: ^{12}C-*Pisolithus* (unlabelled controls) and ^{13}C-*Pisolithus* (labelled samples). The jars were maintained at 20 °C in the dark for 28 days. At each sampling time (Day 0, 7, 14, 21 and 28), 2 g fw of soil was removed from three replicates for each treatment and immediately frozen for subsequent molecular and chemical analyses.

2.2. Soil chemical analysis

Five mg of soil from each sample was used for determining bulk ^{13}C-enrichment by continuous flow isotope ratio mass spectrometry (IRMS) using a Europa Scientific ANCA-NT stable isotope analyser with ANCA-NT Solid/Liquid Preparation Module (Europa Scientific Ltd., Crewe, UK). These data were analysed in Minitab version 15 using General Linear Models (GLM) with jar as a random factor, Differences between time points were analysed by Tukey multiple comparison test. Solid-state nuclear magnetic resonance (NMR) analysis was performed on air dried soil, using a single replicate at each time point, which had been ground to a fine powder. All ^{13}C NMR Cross Polarisation Magic Angle Spinning (CP/MAS) spectra were obtained on a Bruker 200 MHz spectrometer operating at 200 MHz for ^{1}H and 50.3 MHz for ^{13}C. Powdered samples were loaded into 4 mm diameter zirconium oxide rotors with Kel-F caps, and spun at 3.5 kHz. A pulse width of 3.0 μs and a contact time of 0.75 ms were used along with a delay time of 2 s. The number of scans was 8000. All time domain spectra were Fourier transformed with a 150 Hz Lorentzian line broadening to give frequency domain spectra. The chemical shifts were referenced to an external sample of spinning adamantine, with its high frequency signal taken at 37.8 ppm with respect to tetramethylsilane (0 ppm). All NMR spectra were processed using MestRec computer software (Mestrelab Research, Santiago de Compostela, Spain). Absolute signal intensities were normalized by sample weight.

2.3. Nucleic acid extraction and isopycnic centrifugation

DNA was extracted from 0.5 g soil subsamples according to the method previously described by Griffiths et al. (2000) using Bio-101 Multimix matrix tubes and a FastPrep bead beating system (Bio-101, Vista, California, USA) at a speed of 5.5 m s^{-1} for 30 s Nucleic acids were pelleted with two volumes of 30% (w/v) polyethylene glycol 6000 in 1.6 M NaCl for 2 h at room temperature followed by centrifugation at 13,500 rpm for 30 min and washed with cold 70% (v/v) ethanol before being air dried and resuspended in 50 mL of Tris–EDTA buffer (pH 7.4). The integrity and quantity of extracted DNA were checked using NanoDrop, ND-1000 Spectrophotometer (Bio-Rad Laboratories Inc., UK). For all samples, 5 μg of DNA extracts were loaded into a gradient of CsCl (Sigma–Aldrich Inc., St. Louis, MO, USA) of an average density of ~1.72 g mL^{-1} dissolved in gradient buffer (0.1 M Tris–HCl, pH 8; 0.1 M KCl; 1 mM EDTA) (Lueders et al., 2004). Centrifugation was carried out in 4.9 mL polyallomer quick seal tubes in a VTi90 vertical rotor using an Optima L-100 XP ultracentrifuge (Beckman Coulter, Krefeld, Germany). Centrifugations were at 70,000 rpm (133,536 g_{av}) at

20 °C for 36 h. In all, 20 equal fractions (~240 μl) of each gradient were collected from 'heavy' to 'light' using a HPLC syringe pump (B. Braun, Melsuntgen, Germany) and the density of each fraction was determined by weighing the fractions. Each individual gradient fraction was checked for the presence of DNA by agarose gel electrophoresis and DNA was quantified using a NanoDrop 2000 (Thermo Fisher Scientific UK Ltd, Leicestershire, UK). In total, we had 800 individual fractions (20 fractions from each of 40 samples).

2.4. Domain-specific PCR quantification of density-resolved 18S rDNA

Fungal 18S rDNA quantitative PCR (qPCR) was performed to quantify the amount of fungal DNA present in each fraction (800 in total) obtained after density gradient fractionation (Lueders et al., 2004). All qPCRs were performed using the Rotor-Gene SYBR Green PCR Kit on a Rotor-Gene 3000 (Qiagen, Doncaster, VIC, Australia) using the primers Fung5f/FF390r (Lueders et al., 2004) and 40 cycles. All reactions were prepared using a CAS-1200 liquid handling system (Qiagen, Doncaster, VIC, Australia). 18S rDNA standard curves were produced using *Laccaria bicolor* strain S238H82 (accession no.: ABFE00000000; origin: INRA-Nancy, France; Martin et al., 2008) across a DNA concentration range of 10^5 to 10^1. All samples and standards were quantified in at least two different runs to confirm the reproducibility of the quantification. The efficiency of all qPCRs ranged from 90 to 100% ($-3.64 > \text{slope} > -4.31$) and the correlation coefficient (R) was always ≥ 0.99. 18S rDNA qPCR data were analyzed using analysis of variance (ANOVA) with Statistica 9.0 (StatSoft Inc., Tusla, OK). Normality was tested using Shapiro-Wilkins test and the variance of the residuals checked to confirm they were homogenous by Levene's test.

2.5. PCR-denaturing gradient gel electrophoresis (DGGE) analyses

PCR-denaturing gradient gel electrophoresis (DGGE) analyses were performed on each individual ^{12}C- and ^{13}C-density gradient fractions recovered from all samples using the primers ITS1F/ITS4 and ITS1F-GC/ITS2. Unlabelled samples taken from jars containing ^{12}C-mycelium were included for comparison. All PCRs were performed using the conditions described in Anderson et al. (2003) with Go-Taq Flexi DNA polymerase (Promega, Madison, WI, USA). Cycling conditions consisted of 94 °C for 5 min followed by 35 cycles of 94 °C for 30 s, 55 °C for 30 s and 72 °C for 30 s with a final elongation step at 72 °C for 5 min. PCR products were examined by standard 1.5% (w/v) agarose electrophoresis for PCR product quantification prior to performing DGGE analysis.

Approximately 0.5 μg of each PCR product was used for DGGE analysis using a D-Code Universal Mutation Detection System (Bio-Rad, Hercules, CA, USA; Anderson et al., 2003). All gradient gels were topped with 10 mL of acrylamide containing no denaturant and electrophoresis was carried out at 60 °C and 200V for 10 min followed by an additional 16 h at 70V. Gels were stained in ethidium bromide and digital images captured using an Imago apparatus (Bio-Rad Laboratories, Gladesville, NSW, Australia). Each sample was assessed in at least two different runs to confirm the reproducibility of the DGGE fingerprint across gels. To facilitate comparative statistical analysis, all gels were combined into a composite image before further analysis using Corel Photo-Paint 12 (Corel Corporation, San Francisco, CA, USA, 2003). Gel images were normalized with respect to the migration pattern comparison using GelCompar II (Applied Maths NV, Sint-Matens-Laten, Belgium). All bands on the gels were scored to create a binary matrix based on presence or absence. These data were subjected to Principal component analysis (PCA) to investigate the variation in the DGGE banding patterns. Samples were plotted along the first (*x*-axis) and second (*y*-axis) principal components. Jaccard's coefficients of similarity were first calculated between samples and used to compute PCA in Canoco version 4.5 (Ter Braak and Šmilauer, 2002). The PCA axes were treated as "species" data.

2.6. Cloning and sequencing of individual ITS-DGGE bands

Excised DGGE bands were re-amplified using the primers ITS1F (Gardes and Bruns, 1993) ITS2 (White et al., 1990). Purified PCR products (Mobio 96 well ultraclean, Mobio, Carlsbad, California, USA) were cloned into the pGEM-T vector (Promega, Madison, WI, USA) and transformed into *Escherichia coli* JM109 competent cells as per the manufacturer's protocol. Clones (250 in total) with confirmed inserts of the expected size were randomly selected for sequencing using the vector-encoded universal T7 primer (Macrogen, Seoul, Korea). Three different colonies with the expected insert were sequenced to confirm reliability of sequences. Purified PCR products derived from excised DGGE bands were also sent for direct sequencing. Sequences were aligned in the Bioedit Sequence Alignment Editor program (www.mbio.ncsu.edu/BioEdit/bioedit.html). All full length and cloned internal transcribed spacer (ITS) sequences were compared with sequences in public databases by using National Centre for Biotechnology Information (NCBI) Blast (http://www.ncbi.nlm.nih.gov/blast) nucleotide database collection (excluding uncultured fungus sequences). All the sequences were submitted to NCBI with accession numbers JQ513890-JQ513907.

3. Results

3.1. Determination of ^{13}C loss by IRMS and chemical shifts by NMR

IRMS analyses of soils collected at Days 0, 7, 14, 21 and 28 showed a gradual decline in soil ^{13}C content (Fig. 1). There was a *ca* 48% reduction in soil ^{13}C content from Day 0 to Day 28 with the largest reduction (33%) occurring in the first 7 days immediately after incorporation of the ^{13}C-labelled *P. microcarpus* necromass to the pots (Fig. 1).

The CP-MAS ^{13}C NMR spectra comprised distinct peaks representing six key functional groups containing C (Table 1). The

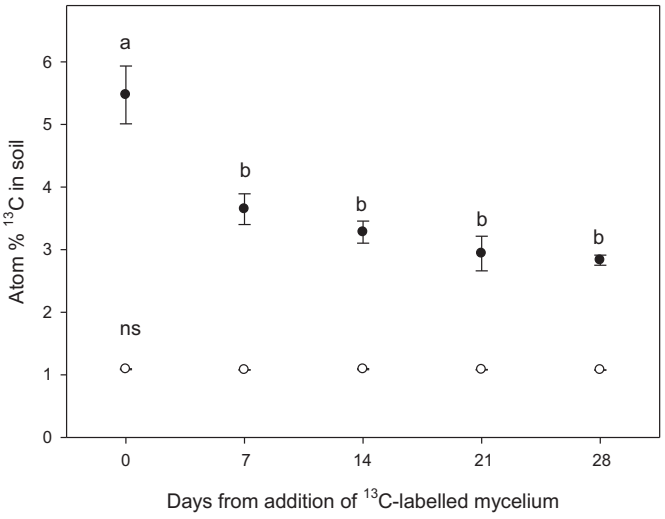

Fig. 1. Atom % ^{13}C of bulk soil that received ^{13}C-labelled mycelium (solid symbols) or unlabelled mycelium (open symbols) sampled at the time of addition (Day 0) and every week thereafter (±SEM). Bars sharing a letter are not significantly different ($P > 0.001$). There were no significant (ns) differences among sampling dates for unlabelled soils; note that error bars fall within confines of points in many instances.

Table 1
Chemical shift assignments of resonances in the CP-MAS ^{13}C NMR spectra of soil incubated with ^{13}C-labelled *Pisolithus microcarpus* mycelial necromass.

Functional groups	^{13}C NMR chemical shift (ppm)	Assignment of possible source(s)
C=O-	174.7	Carbonyl carbon of chitin, proteins and lipids
O-(CH)n-O	102.4	C_1anomeric carbon in glycogen and chitin-glucan
O-alkyl C	72.7 (broad)	C_3, C_4 and C_5 carbon in glycogen and chitin-glucan
O-alkyl C	61.4	C_2 and C_6 carbon in glycogen and chitin-glucan
$(CH_2)n$	30.6	Aliphatic carbons of polymethylene and lipids
CH_3	22.4	Methyl carbon of chitin and lipids

^{13}C NMR spectra were different to those reported for chitin (Kameda et al., 2005) but showed similarities to the spectra for glycogen (Serafim et al., 2002) and the chitin/glucan complex (Kameda et al., 2005). The peaks corresponding to C_2 is expected at about 55 ppm, however, this peak was not resolved and appeared as a shoulder to a broad peak at 61.4 ppm corresponding to C_6 of chitin-glucan and glycogen. Similarly, the broad peak at 72.7 ppm corresponded to O-alkyls of C_3, C_4 and C_5 for chitin-glucan and glycogen appeared as the most intense peak in the spectrum. The relative abundance of the six functional groups decreased throughout the incubation period (Fig. 2). In particular, there was rapid loss of the peak intensity at 72.7 ppm during the first week of incubation, a pattern that was also seen, albeit to a lesser extent, in the other functional groups. After the first week, the major contribution to the NMR spectrum was from the functional groups with O-alkyl and the polymethylene C. The intensity of the peaks corresponding to lipids, such as carbonyl peak at 174.7 ppm and the methyl peak at 22.4 ppm were relatively dominant compared to the anomeric C_1 peak at 102.4 ppm. Because both the IRMS data showed very little change in ^{13}C content between Day 21 and 28, and the NMR data showed very little change in the key functional groups between Days 14 and 28, only soil samples from Day 0, 7, 14 and 21 were included in the molecular analyses.

3.2. Distribution of ^{12}C- and ^{13}C-labelled DNA in CsCl gradients

The use of identical unlabelled control samples allowed us to unequivocally identify the density at which ^{12}C- and ^{13}C-DNA occurred in the CsCl gradient. Using real-time PCR, only a single 18S rDNA peak (5×10^7 copies) was detected in the unlabelled control samples. This occurred at a buoyant density of 1.68 g mL^{-1} (Fig. 3a). In contrast, in the samples that received ^{13}C-labelled mycelium, two peaks were detected at each sampling time point (i.e. Days 7, 14 and 21). One of these occurred at a buoyant density of 1.68 g mL^{-1} while the other was at 1.83 g mL^{-1} (Fig. 3a). We therefore considered the fractions corresponding to buoyant densities of 1.66–1.69 g mL^{-1} (3 out of 20 fractions) to represent unlabelled (i.e. ^{12}C) DNA and those fractions at buoyant densities of 1.82–1.85 g mL^{-1} (3 out of 20 fractions) to represent labelled (i.e. ^{13}C) DNA. In both the ^{12}C-unlabelled and ^{13}C-labelled fractions there was a decline in 18S rDNA gene copies from soil samples taken at Day 7 to Day 14 and 21 (Fig. 3b), indicating a decrease in both ^{12}C-unlabelled and ^{13}C-labelled fungal DNA over the time course of the experiment.

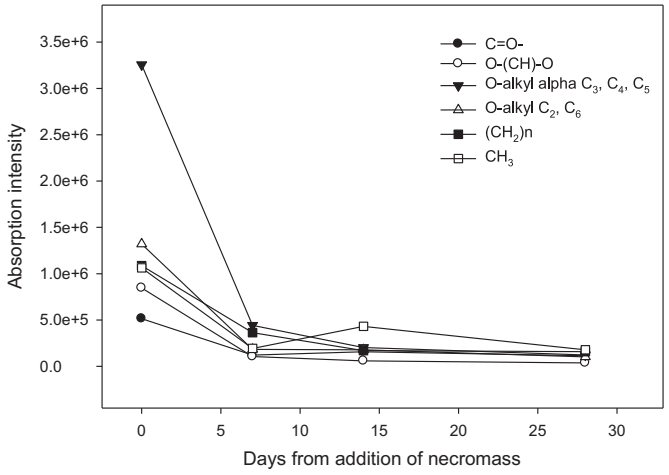

Fig. 2. Variation in the ^{13}C NMR peak intensities of different chemical functional groups in soil samples incubated for 28 days with ^{13}C-labelled fungal mycelium.

3.3. ITS-DGGE and sequence analyses

ITS-DGGE banding patterns derived from the ^{13}C-DNA fractions at Day 7, 14 and 21 were significantly different ($P < 0.001$) from those observed at Day 0 (^{12}C-DNA; Fig. 4 & S1). The first ordination axis, which explained 40.5% of the variability in taxon composition, revealed a clear separation of fungal community structure in the ^{13}C-enriched fractions of rDNA extracts at Day 7, 14 and 21 (Fig. 4). Specific fungal community members, represented by individual ITS-DGGE bands within the ^{12}C- and ^{13}C-DNA-based profiles, were subsequently identified by direct sequencing of excised DGGE bands and by sequencing clones from libraries constructed from ^{12}C- to ^{13}C centrifugation gradient fractions at each sampling time (Day 0, 7, 14 and 21; Table 2). Significant differences ($P < 0.001$), generated by comparing the ^{12}C- and ^{13}C-DGGE patterns via PCA

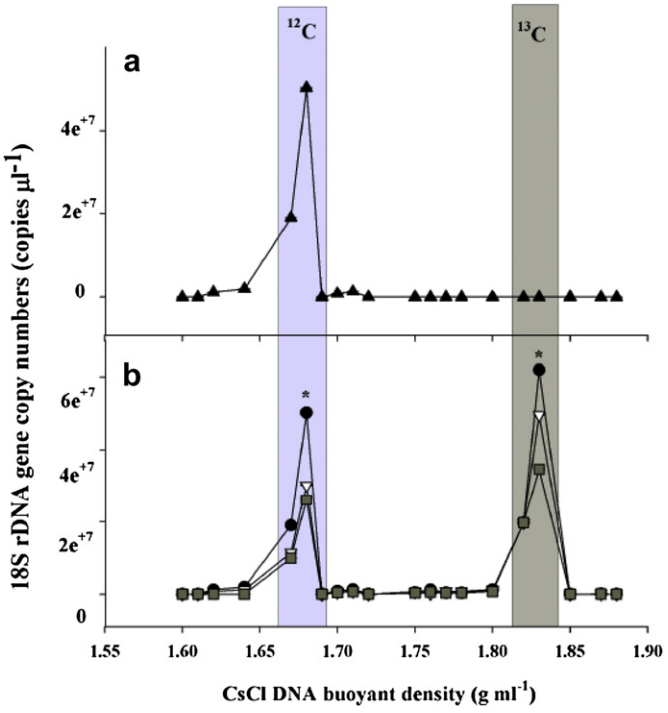

Fig. 3. Quantification of 18S rDNA gene copy number throughout CsCl density gradients (±SEM). DNA was extracted from soil at (a) Day 0 (unlabelled control), and (b) Day 7 (●), 14 (○) and 21 (▼) after incubation with ^{13}C-labelled *Pisolithus microcarpus* mycelial necromass. Fungal SSU rRNA template distribution within the gradient fractions was quantified with real-time PCR. The densities of the 'heavy' ^{13}C-rDNA and 'light' ^{12}C-rDNA are shaded in grey. All the density separated fractions were used for the PCR-DGGE fingerprinting analysis. In (b), * indicates an overall significant ($P < 0.001$) effect of sample date within both heavy and light fractions.

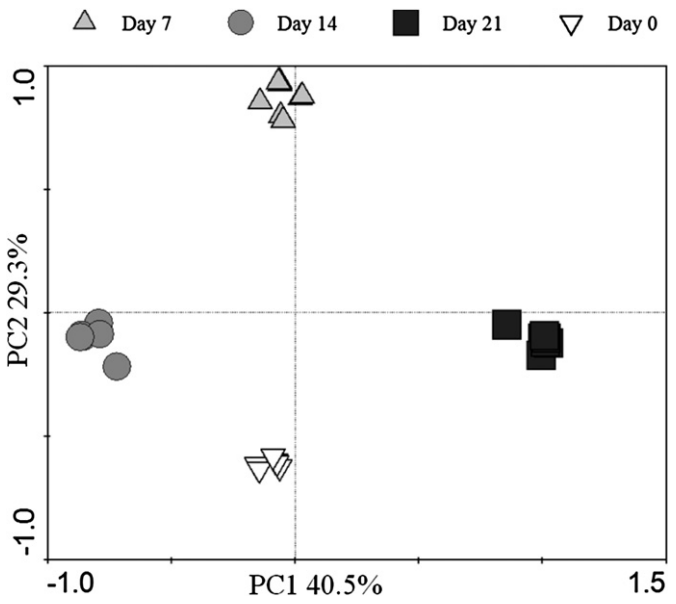

Fig. 4. Principal component analysis of fungal communities generated by DGGE analysis of the ITS region from rDNA extracted from 'non-active' (Day 0; ^{12}C) and 'active' (Day 7, 14 and 21; ^{13}C) density fractions.

(Fig. 4), were confirmed by analyses of the sequence data (Table 2). The sequences generated from ^{13}C-DNA fractions represented a subset of the diversity found in the ^{12}C-DNA.

4. Discussion

Here we report the first application of DNA-SIP to trace C from decaying ECM fungal mycelium into the soil fungal community. Whilst $^{13}CO_2$ pulse labelling approaches have been used to trace C flow from plant photosynthesis into physiologically active fungi in the rhizosphere of herbaceous plants (Olsson and Johnson, 2005; Vandenkoornhuyse et al., 2007; Drigo et al., 2010), these approaches do not enable identification of the key microorganisms involved in decomposition of mycelium or enable C transfer from root and mycorrhizal fungal pathways to be separated. It is also technically difficult to ensure that $^{13}CO_2$ delivered to plants can be detected in the mycorrhizosphere because of the effects of dilution of the added isotope. Thus, we advocate the use of ^{13}C-labelled substrates, such as mycelium, to complement $^{13}CO_2$ approaches in order to better understand this specific pathway of C flux from plants to soils.

Our analysis identifies groups of fungi that can rapidly utilise C from decomposing ECM mycelium. As revealed by DGGE and sequencing analyses, we found that Basidiomycete fungi were the principal group involved in the incorporation of C into biomass from labelled mycelium throughout the short-term incubation. Identification of sequences closely related to known mycorrhizal genera such as *Laccaria* and *Lactarius* in the absence of host plants is interesting and suggests that the fungi from which the sequences originated may have limited saprotrophic abilities, at least throughout the short time-frame of our incubation study. The increasing proportion of basidiomycetes versus ascomycetes throughout the incubation may reflect preferential utilisation of secondary compounds or shifts in the competitive abilities between different fungi. The data also highlight a fine-scale temporal dynamic of ^{13}C utilisation, which may be a result of competition from other microbial groups through time, the preferential utilisation of specific components of the necromass, and disruption in niche caused by sub-sampling. An essential aspect of the experimental design was the use of identical unlabelled substrates as controls to permit unequivocal identification of ^{13}C incorporation over and above potential experimental artefacts (e.g. migration of DNA down centrifuge tubes according to their GC content). Given the level of enrichment observed in our study, RNA-SIP may also be feasible (Drigo et al., 2010). This approach may have greater ability to determine more rapid responses in the composition of the active microbial community and open up possibilities to target functional genes that may be involved in C transformation or assimilation/uptake processes.

Our findings demonstrate that components of EMM can turnover very rapidly and therefore have potential to be important sources of both mineral nutrients and C flux in dry sclerophyll forests. Given the vast quantity of EMM produced by most species of ECM fungi and the subsequently large standing biomass (Wallander et al., 2001), remarkably little is known about the dynamics of hyphal turnover in soil and the organisms involved in its decomposition. The incorporation of ^{13}C into microbial taxa combined with loss of ^{13}C from glycogen and chitin-glucan

Table 2
Characterisation of ITS rDNA PCR products from the 'light' (^{12}C-DNA) and 'heavy' (^{13}C-DNA) fractions. Sequences were retrieved from bands excised from the $^{12}C/^{13}C$-DNA-based DGGE (refer to Fig. S1 for locations of bands on the gel) and from clone libraries. + refers to the presence of sequences and − to their absence. The taxonomic affiliation is according to closest neighbours in the GenBank database.

Family	Closest match (accession no./% similarity)	Band on gel	^{12}C-DNA 0 days	^{13}C-DNA		
				7 days	14 days	21 days
Tremellales	*Cryptococcus podzolicus* (FN428924/98%)	4	+	+	+	+
Trichosporonaceae	*Trichosporon mucoides* (AM159634/100%)	6	+	+	+	+
Helotiaceae	*Uncultured rhizoscyphus* (GU998109.1/97%)	9	+	+	+	+
Tricholomataceae	*Laccaria* sp. (DQ499640.1/95%)	12	+	+	+	+
Myxotrichaceae	*Uncultured Oidiodendron* (GQ338892/100%)	13	+	+	+	+
Russulaceae	*Lactarius fennoscandius* (DQ922534/95%)	14	+	+	+	+
Clavicipitaceae	*Mariannaea camptospora* (EU551206/99%)	15	+	+	+	+
–	*Uncultured basidiomycete* (FJ456968/100%)	16	+	+	+	+
Chaetosphaeriaceae	*Chloridium virescens* (EF029220/97%)	17	+	+	+	+
Sclerodermataceae	*Pisolithus microcarpus* (HQ693102/100%)	18	+	+	+	+
Davidiellaceae	*Cladosporium sphaerospermum* (AM159631/100%)	7	+	+	+	−
–	*Uncultured leotiomyceta* (HQ211906/100%)	5	+	−	+	−
–	*Uncultured mycorrhiza* (EF558820/98%)	8	+	−	+	−
–	*Uncultured fungus* (FN611001.1/100%)	1	+	−	+	−
Cystofilobasidiaceae	*Mrakia* sp. (AY038833/100%)	10	+	−	+	−
Trichosporonaceae	*Trichosporon dulcitum* (GQ222351/100%)	11	+	−	+	+
Tricholomataceae	*Tricholoma* sp. (AF377179/98%)	2	+	−	−	+
Nectriaceae	*Neonectria radicicola* (GQ131874/98%)	3	+	−	−	+

complexes (from the NMR data), suggests a rapid loss of labile C in the very early stages of decomposition. We also captured CO_2 released from the jars in sodium hydroxide vials and the ^{13}C-enrichment of these samples (which was too high to quantify with IRMS so data not shown) also provides further support for a rapid initial loss of C, rather than complete transfer into other pools. Past work using ^{14}C-labelled fungi has determined that the rate of decomposition of fungal fractions declines in the order cytoplasm, cell walls and melanin (Malik and Hader, 1982). The combined use of NMR permits more sophisticated parallel analysis of changes in specific chemical groups; these data suggest that glycogen breaks down quickly when mycelium dies. Glycogen is recognised as having a key role in the C cycle at the plant:fungus interface (Smith and Read, 2008). Early experiments using excised beech mycorrhizas demonstrated that glucose is rapidly converted to form glycogen which accumulates in fungal tissue, where the total insoluble carbohydrate fraction (which likely comprises mostly glycogen) is around 17% of the total carbohydrate content (Lewis and Harley, 1965). Subsequent cytochemical studies have confirmed that glycogen accumulates as formation of ectomycorrhizas proceeds (Jordy et al., 1998). The chemical profile of the NMR spectrum after four weeks contained lipids as the major component with minor amounts of chitin-glucan complexes. These complexes are thought to be ubiquitous in fungi (Siestma and Wessels, 1979), and the production of extra-cellular chitinolytic enzymes by soil microorganisms in forests is well established (e.g. Gray and Baxby, 1968; Baldrian et al., 2011). The abundance of lipids confirms that they undergo slow degradation compared to glycogen. The absence of a ^{13}C NMR resonance at 94 ppm suggests that the samples did not contain anomeric C_1 corresponding to trehelose, a disaccharide found in spores of many organisms including fungi (Gil et al., 1996).

The extent to which rapid turnover of hyphal C occurs in the field under more natural circumstances needs to be determined. For example, we grew our fungi on MMN until optimal conditions and this may have affected the composition of C sources in the mycelium, although as noted previously key compounds like glycogen are found in intact ectomycorrhizas (Jordy et al., 1998). In addition, the mycelium was lightly macerated in our study in order to maximise incorporation of ^{13}C into nucleic acids and homogenise the material. Whether light maceration would stimulate autolysis of hyphae is unclear. Previous experiments have shown that autolysis of both dead and live fungal hyphae of some, but not all, species can occur in soil (Lloyd and Lockwood, 1966). More recent work has shown that between 20 and 80% of the mass of intact mycelium from pure cultures is lost within a month after addition to soils (Koide and Malcolm, 2009) and that saprotrophic fungi (based on analysis of DNA) proliferate in response to inputs of external mycelium (Lindahl et al., 2010), which provides support for our findings that C is rapidly utilised by opportunistic fungi, and probably other microbes, in nature. Our data also concur with recent findings demonstrating that additions to soil of dead ECM mycelium rapidly stimulated CO_2 efflux from free-living soil microbes (Wilkinson et al., 2011). The application of SIP to these sorts of experiments may be an ideal tool to understand the mechanisms behind their findings that species richness of hyphal necromass mediates CO_2 release. Further evidence of rapid turnover of ECM fungi comes from intensive temporal and spatial sampling which has shown that ECM fungal communities can be highly dynamic with considerable among-year variation in the numbers, distribution and identity of ECM root tips (Pickles et al., 2010).

The amount of hyphae added (7.25 mg dwt g^{-1} soil) is at the upper end of most estimates of mycelial standing biomass (Wallander et al., 2001), but considerably less than the amount of mycelium found in ECM mats, for example (Ingham et al., 1991). We also focused on diffuse hyphae rather than rhizomorphs, and whilst the MMN growth medium that we used is comparatively nutrient poor, it nevertheless results in fungal colonies with uniform nutrient content. Little is known about the nutritional state of ECM fungal hyphae as it senesces in nature but one could speculate that there may be a degree of nutrient resorption before mycelium enters soil as necromass. On the other hand, grazing and incidental disruption of ECM hyphae by invertebrates (Setala, 2000) may result in sections of intact mycelial networks becoming detached from host plants and dying before such remobilisation processes occur. In many ECM fungi, hyphae aggregate to form rhizomorphs that are typically hydrophobic and long-lived (e.g. Agerer, 2001). In a laboratory study of *Pisolithus tinctorius* in symbiosis with *Pinus taeda* seedlings, the rhizomorphs contributed to only 7% of the length of the mycelium but their dry matter was twice that of the diffuse mycelium (Rousseau et al., 1994). The proportion of rhizomorphs versus diffuse hyphae will probably impact on the turnover rate of external mycelium. Rhizomorphs have been shown to have mean life times ranging from 7 to 22 months and some can survive over several growing seasons (Treseder et al., 2005; Pritchard et al., 2008). Nevertheless, our experiment paves the way for future applications of SIP using intact hyphae, which would inevitably be less enriched in ^{13}C than the mycelium we used, to identify key organisms actively utilising decaying external mycelium as energy sources.

Acknowledgements

We thank Nathalie Curlevski, Duncan White and Barry Thornton for technical assistance, Francis Martin for providing the *Laccaria bicolor* strain S238H82 and Alan McCutcheon for carrying out the NMR spectroscopic studies. This work was supported by a New South Wales Office for Science and Medical Research – Life Sciences Research Award, an Australian Research Council Linkage International awards (gs1) grant, and a UK Natural Environment Research Council Advanced Fellowship. We also thank the University of Western Sydney, College of Health and Science for their collaborative research initiative funding.

Appendix. Supplementary data

Supplementary data associated with this article can be found, in the online version, at doi:10.1016/j.soilbio.2012.02.003.

References

Agerer, R., 2001. Exploration types of ectomycorrhizae. A proposal to classify ectomycorrhizal mycelial systems according to their patterns of differentiation and putative ecological importance. Mycorrhiza 11, 107–114.

Anderson, I.C., Campbell, C.D., Prosser, J.I., 2003. Diversity of fungi in organic soils under a moorland – Scots pine (*Pinus sylvestris* L.) gradient. Environmental Microbiology 5, 1121–1132.

Bååth, E., Nilsson, L.-O., Goransson, H., Wallander, H., 2004. Can the extent of degradation of soil fungal mycelium during soil incubation be used to estimate ectomycorrhizal biomass in soil? Soil Biology and Biochemistry 36, 2105–2109.

Baldock, J.A., Oades, J.M., Vassallo, A.M., Wilson, M.A., 1990. Significance of microbial activity in soils as demonstrated by solid-state ^{13}C NMR. Environmental Science and Technology 24, 527–530.

Baldrian, P., Voříšková, J., Dobiášová, P., Merhautová, V., Lisá, L., Valášková, V., 2011. Production of extracellular enzymes and degradation of biopolymers by saprotrophic microfungi from the upper layers of forest soil. Plant and Soil 338, 111–125.

Bastias, B.A., Anderson, I.C., Rangel-Castro, J.I., Parkin, P.I., Prosser, J.I., Cairney, J.W.G., 2009. Influence of repeated prescribed burning on incorporation of ^{13}C from cellulose by forest soil fungi as determined by RNA stable isotope probing. Soil Biology and Biochemistry 41, 467–472.

Beiler, K.J., Durall, D.M., Simard, S.W., Maxwell, S.A., Kretzer, A.M., 2008. Architecture of the wood-wide web: *Rhizopogon* spp. genets link multiple Douglas-fir cohorts. New Phytologist 185, 543–553.

Chigineva, N.I., Aleksandrova, A.V., Tiunov, A.V., 2009. The addition of labile carbon alters litter fungal communities and decreases litter decomposition rates. Applied Soil Ecology 42, 264–270.

Cleveland, C.C., Nemergut, D.R., Schmidt, S.K., Townsend, A.R., 2007. Increases in soil respiration following labile carbon additions linked to rapid shifts in soil microbial community composition. Biogeochemistry 82, 229–240.

Drigo, B., van Veen, J.A., Pijl, A.S., Kielak, A.M., Gamper, H.A., Houtekamer, M.J., Boschker, H.T.S., Bodelier, P.L.E., Whiteley, A.S., Kowalchuk, G.A., 2010. Shifting carbon flow from roots into associated microbial communities in response to elevated atmospheric CO_2. Proceedings of the National Academy of Sciences of the USA 107, 10938–10942.

Fan, T.W.M., Bird, J.A., Brodie, E.L., Lane, A.N., 2009. ^{13}C Isotopomer based metabolomics of microbial groups isolated from two forest soils. Metabolomics 5, 108–122.

Gardes, M., Bruns, T.D., 1993. ITS primers with enhanced specificity for basidiomycetes – application to the identification of mycorrhizae and rusts. Molecular Ecology 2, 113–118.

Gil, A.M., Belton, P.S., Felix, V., 1996. Spectroscopic studies of solid alpha-alpha trehalose. Spectrochimica Acta Part A 52, 1649–1659.

Godbold, D.L., Hoosbeek, M.R., Lukac, M., Cotrufo, M.F., Janssens, I.A., Ceulemans, R., Polle, A., Velthorst, E.J., Scarascia-Mugnozza, G., De Angelis, P., Miglietta, F., Peressotti, A., 2006. Mycorrhizal hyphal turnover as a dominant process for carbon input into soil organic matter. Plant and Soil 281, 15–24.

Gray, T.R.G., Baxby, P., 1968. Ecology of chitinocalstic micro-organisms in forest soil. Transactions of the British Mycological Society 51, 293–298.

Griffiths, R.I., Whiteley, A.S., O'Donnell, A.G., Bailey, M.J., 2000. Rapid method for coextraction of DNA and RNA from natural environments for analysis of ribosomal DNA- and rRNA-based microbial community composition. Applied and Environmental Microbiology 66, 5488–5491.

Heinemeyer, A., Hartley, I.P., Evans, S.P., De la Fuente, J.A.C., Ineson, P., 2007. Forest soil CO_2 flux: uncovering the contribution and environmental responses of ectomycorrhizas. Global Change Biology 13, 1786–1797.

Heux, L., Brugnerotto, J., Desbrieres, J., Versali, M.F., Rinaudo, M., 2000. Solid state of NMR for determination of degree of acetylation of chitin and chitosan. Biomacromolecules 1, 746–751.

Högberg, M.N., Högberg, P., 2002. Extramatrical ectomycorrhizal mycelium contributes one-third of microbial biomass and produces, together with associated roots, half the dissolved organic carbon in a forest soil. New Phytologist 154, 791–795.

Ingham, E.R., Griffiths, R.P., Cromack, K., Estry, J.A., 1991. Comparison of direct vs. fumigation incubation microbial biomass estimates from ectomycorrhizal mat and non-mat soils. Soil Biology and Biochemistry 23, 465–471.

Jordy, M.N., Azémar-Lorentz, S., Brun, A., Botton, B., Pargney, J.C., 1998. Cytolocalization of glycogen, starch, and other insoluble polysaccharides during ontogeny of Paxillus involutus-Betula pendula ectomycorrhizas. New Phytologist 140, 331–341.

Kameda, T., Miyazawa, M., Ono, H., Yoshida, M., 2005. Hydrogen bonding structure and stability of a-chitin studied by ^{13}C solid-state NMR. Macromolecular Bioscience 5, 103–106.

Kennedy, P., 2010. Ectomycorrhizal and interpecific competition: species interactions, community structure, coexistence mechanisms and future research directions. New Phytologist 187, 895–910.

Koide, R.T., Malcolm, G.M., 2009. N concentration controls decomposition rates of different strains of ectomycorrhizal fungi. Fungal Ecology 2, 197–202.

Leake, J.R., 2001. Is diversity of ectomycorrhizal fungi important for ecosystem function? New Phytologist 152, 1–3.

Leake, J.R., Johnson, D., Donnelly, D.P., Muckle, G.E., Boddy, L., Read, D.J., 2004. Networks of power and influence: the role of mycorrhizal mycelium in controlling plant communities and agroecosystem functioning. Canadian Journal of Botany 82, 1016–1045.

Lee, C.G., Watanabe, T., Sato, Y., Murase, J., Asakawa, S., Kimura, M., 2011. Bacterial populations assimilating carbon from ^{13}C labelled plant residue in soil: analysis by DNA-SIP approach. Soil Biology and Biochemistry 43, 814–822.

Lewis, D.H., Harley, J.L., 1965. Carbohydrate physiology of mycorrhizal roots of beech. I. Identity of endogenous sugars and utilization of exogenous sugars. New Phytologist 64, 224–237.

Lindahl, B.D., de Boer, W., Finlay, R.D., 2010. Disruption of root carbon transport into forest humus stimulates fungal opportunists at the expense of mycorrhizal fungi. International Society for Microbial Ecology Journal 4, 872–881.

Lloyd, A.B., Lockwood, J.L., 1966. Lysis of fungal hyphae in soil and its possible relations to autolysis. Phytopathol 56, 595–602.

Lueders, T., Pommerenke, B., Friedrich, M.W., 2004. Stable-isotope probing of microorganisms thriving at thermodynamic limits: syntrophic propionate oxidation in flooded soil. Applied and Environmental Microbiology 70, 5778–5786.

Malik, K.A., Hader, K., 1982. Decomposition of ^{14}C-labeled melanoid fungal residues in a marginally sodic soil. Soil Biology and Biochemistry 14, 457–460.

Martin, F., Aerts, A., Ahren, D., Brun, A., Danchin, E.G.J., Duchaussoy, F., Gibon, J., Kohler, A., Lindquist, E., Pereda, V., et al., 2008. The genome of *Laccaria bicolor* provides insights into mycorrhizal symbiosis. Nature 452, 88–92.

Marx, D.H., 1969. The influence of ectotrophic mycorrhizal fungi on the resistance of pine roots to pathogenic infections. I. Antagonism of mycorrhizal fungi to root pathogenic fungi and soil bacteria. Phytopathology 59, 153–163.

Olsson, P.A., Johnson, N.C., 2005. Tracking carbon from the atmosphere to the rhizosphere. Ecology Letters 8, 1264–1270.

Pickles, B.J., Genney, D.R., Potts, J.M., Lennon, J.J., Anderson, I.C., Alexander, I.J., 2010. Spatial and temporal ecology of Scots pine mycorrhizas. New Phytologist 186, 755–768.

Pritchard, S.G., Strand, A.E., McCormack, M.L., Davis, M.A., Oren, R., 2008. Mycorrhizal and rhizomorph dynamics in a loblolly pine forest during 5 years of free-air-CO_2-enrichment. Global Change Biology 14, 1–13.

Radajewski, S., Ineson, P., Parekh, N.R., Murrell, J.C., 2000. Stable-isotope probing as a tool in microbial ecology. Nature 403, 646–649.

Rousseau, J.V.D., Sylvia, D.M., Fox, A.J., 1994. Contribution of ectomycorrhiza to the potential nutrient-absorbing surface of pine. New Phytologist 128, 639–644.

Serafim, L.C., Lemos, P.C., Levantesi, C., Tandoi, V., Santos, H., Reis, M.A.M., 2002. Methods for detection and visualization of intracellular polymers stored by polyphosphate-accumulating microorganisms. Journal of Microbiological Methods 51, 1–18.

Setala, H., 2000. Reciprocal interactions between Scots pine and soil food web structure in the presence and absence of ectomycorrhiza. Oecologia 125, 109–118.

Siestma, J.H., Wessels, J.G.H., 1979. Evidence for covalent linkages between chitin and beta-glucan in a fungal wall. Journal of General Microbiology 114, 99–108.

Smith, S.E., Read, D.J., 2008. Mycorrhizal Symbiosis, third ed. Academic Press.

Ter Braak, C.J.F., Šmilauer, P., 2002. CANOCO Reference Manual and CanoDraw for Windows User's Guide: Software for Canonical Community Ordination (Version 4.5). Microcomputer Power, Ithaca, NY.

Treseder, K.K., Allen, M.F., Ruess, R.W., Pregitzer, K.S., Hendrick, R.L., 2005. Lifespans of fungal rhizomorphs under nitrogen fertilization in a pinyon-juniper woodland. Plant and Soil 270, 249–255.

Vandenkoornhuyse, P., Mahe, S., Ineson, P., Staddon, P., Ostle, N., Cliquet, J.B., Francez, A.J., Fitter, A.H., Young, J.P.W., 2007. Active root-inhabiting microbes identified by rapid incorporation of plant-derived carbon into RNA. Proceedings of the National Academy of Sciences of the USA 104, 16970–16975.

Wallander, H., Nilsson, L.O., Hagerberg, D., Bååth, E., 2001. Estimation of the biomass and production of external mycelium of ectomycorrhizal fungi in the field. New Phytologist 151, 753–760.

Wallander, H., Göransson, H., Rosengren, U., 2004. Production, standing biomass and natural abundance of ^{15}N and ^{13}C in ectomycorrhizal mycelia collected at different soil depths in two forest types. Oecologia 139, 89–97.

White, T.J., Bruns, T.D., Lee, S., Taylor, J.W., 1990. Amplification and direct sequencing of fungal ribosomal RNA genes for phylogenetics. In: Innis, M.A., Gelfand, D.H., Sninsky, J.J., White, T.J. (Eds.), PCR Protocols: A Guide to Methods and Applications. Academic Press, London, UK, pp. 315–322.

Wilkinson, A., Alexander, I.J., Johnson, D., 2011. Species richness of ectomycorrhizal hyphal necromass stimulates soil CO_2 efflux. Soil Biology and Biochemistry 43, 1350–1355.